SIAM J. NUMER. ANAL.
Vol. 41, No. 6, pp. 2233–2261

NUMERICAL DISCRETIZATION OF BOUNDARY CONDITIONS FOR FIRST ORDER HAMILTON–JACOBI EQUATIONS*

RÉMI ABGRALL†

Abstract. We provide two simple ways of discretizing a large class of boundary conditions for first order Hamilton–Jacobi equations. We show the convergence of the numerical scheme under mild assumptions. However, many types of such boundary conditions can be written in this way. Some provide "good" numerical results (i.e., without boundary layers), whereas others do not. To select a good one, we first give some general results for monotone schemes which mimic the maximum principle of the continuous case, and then we show in particular cases that no boundary layer can exist. Some numerical applications illustrate the method. An extension to a geophysical problem is also considered.

Key words. Hamilton–Jacobi equations, approximation of boundary conditions

AMS subject classifications. 65M60, 65N99, 35L60, 65Z05, 35Q58

DOI. 10.1137/S0036142998345980

1. Introduction.

The problem of discretizing first order Hamilton–Jacobi equations in $\mathbb{R}^N$ has been considered by several authors (see, e.g., [8, 9, 3]) on various types of meshes (see the previous references and [1]). However, in our knowledge, the discretization of boundary conditions has not yet been considered in a systematic way. The aim of this paper is to provide a simple and systematic way of discretizing a wide variety of boundary conditions. This is done in the framework of discontinuous viscosity solutions [4]. More precisely, we consider the following problem:

$$\begin{cases} H(x,u,Du)=0, & x\in\Omega,\\ F(x,u,Du)=0, & x\in\partial\Omega, \end{cases} \tag{1.1}$$

where the Hamiltonian is continuous on $\overline{\Omega}\times\mathbb{R}\times\mathbb{R}^N$ and the boundary condition F is continuous on $\partial\Omega\times\mathbb{R}\times\mathbb{R}^N$.

For any function z, we consider the upper semicontinuous (u.s.c) and lower semicontinuous (l.s.c) envelopes of z with respect to all variables. These are defined by

$$z^*(x)=\limsup_{x\to y} z(y) \quad \text{and} \quad z_*(x)=\liminf_{x\to y} z(y).$$

Following [4], we introduce the function G:

$$G(x,u,p)=\begin{cases} H(x,u,p), & x\in\Omega,\\ F(x,u,p), & x\in\partial\Omega. \end{cases}$$

A locally bounded u.s.c function u defined on $\overline{\Omega}$ is a viscosity subsolution of (1.1) if and only if, for any $\phi\in C^1(\overline{\Omega})$, if $x_0\in\overline{\Omega}$ is a local maximum of $u-\phi$, then

$$G_*(x_0,u(x_0),D\phi(x_0))\le 0. \tag{1.2}$$

*Received by the editors October 12, 1998; accepted for publication (in revised form) March 31, 2003; published electronically December 5, 2003. This research was supported in part by D.O.E grant DE–FG02–88ER25053 when the author was at the Courant Institute, on leave from INRIA Sophia Antipolis, then during a visit at RIACS, NASA Ames Research Center, Moffett Field, CA.
http://www.siam.org/journals/sinum/41-6/34598.html

†Mathématiques Appliquées de Bordeaux, Université Bordeaux I, 351 Cours de la Libération, 33 405 Talence cedex, France, and Institut Universitaire de France (abgrall@math.u-bordeaux.fr).

Similarly, u, a locally bounded l.s.c. function defined on $\overline{\Omega}$, is a viscosity supersolution of (1.1) if and only if, for any $\phi \in C^1(\overline{\Omega})$, if $x_0 \in \overline{\Omega}$ is a local minimum of $u - \phi$, then

$$G^*(x_0, u(x_0), D\phi(x_0)) \geq 0. \tag{1.3}$$

The computation of G_* and G^* is easy, and we have

$$\begin{cases} G_*(x,u,p) = G^*(x,u,p) = H(x,u,p) & \text{if } x \in \Omega, \\ G_*(x,u,p) = \min(H(x,u,p), F(x,u,p)) & \text{if } x \in \partial\Omega, \\ G^*(x,u,p) = \max(H(x,u,p), F(x,u,p)) & \text{if } x \in \partial\Omega. \end{cases} \tag{1.4}$$

More specifically, we consider the cases of the Dirichlet and Neumann boundary conditions, but the results of this paper may extend to more general boundary conditions, provided they are of the form (1.1) and if some regularity on F is assumed. In the case of Dirichlet boundary conditions, namely $u = \varphi$, we have

$$F(x,u,p) = u(x) - \varphi(x), \tag{1.5}$$

and for Neumann boundary conditions we have

$$F(x,u,p) = \frac{\partial u}{\partial n} - g(x), \tag{1.6}$$

where g is defined on $\partial\Omega$ and continuous.

This paper is organized as follows. We first recall a convergence result by Barles and Souganidis [5]. Then, starting from the dynamical programming principle, we indicate a way of discretizing general boundary conditions, and show the convergence of this scheme. In a second part, we describe several particular cases for convex and nonconvex Hamiltonians. A particular emphasis is set on the Dirichlet boundary conditions because it is more difficult to provide effective boundary conditions in that case, at least more difficult than for Neumann conditions. This problem is explained and has many similarities with the technical difficulties encountered in the study of these conditions in the continuous case. We provide numerical illustrations that show the effectiveness of the schemes. It is known that first order Hamilton–Jacobi equations have many similarities with a particular class of hyperbolic systems. Because of that, one might think that boundary conditions built on the structure of inflow and outflow characteristics would be efficient enough. This is true if the structure of the solution is known a priori. This is rarely the case in practice, and we provide an example where the structure of the solution at the boundary is not known a priori, so more sophisticated approximations are required. Another example has its origin in seismology problems.

Throughout the paper, we consider an open and bounded domain Ω. To simplify the presentation, we assume $\Omega \subset \mathbb{R}^2$, but our results are also valid for $\mathbb{R}^N$, $N \geq 2$. The open set Ω is discretized by a triangulation $\mathcal{T}_\rho$. The nodes of the mesh are denoted by $x_i, i = 1, \ldots, n_s$; the triangles are denoted by $T_k, k = 1, \ldots, n_T$. The vertices of T are denoted by $x_{i_k}, k = 1, \ldots, 3$. The parameter ρ above is, for example, the largest radius of the circumscribed circles of T_k, $k = 1, \ldots, n_T$.

2. A convergence result.

2.1. Preliminaries. All our results rely on the following one by Barles and Souganidis [5]. The symbol $B(\overline{\Omega})$ denotes the set of bounded functions over $\overline{\Omega}$.

They consider approximations schemes of the form

$$S(\rho, x, u^\rho(x), u^\rho) = 0 \qquad \text{in } \overline{\Omega}, \tag{2.1}$$

where S maps $\mathbb{R}^+ \times \overline{\Omega} \times \mathbb{R} \times B(\overline{\Omega})$ onto $\mathbb{R}$, is locally bounded, and has the following properties:

1. monotonicity: if $u \geq v$, for all $\rho \geq 0$, $x \in \overline{\Omega}$, $t \in \mathbb{R}$, and $u, v \in L^\infty(\overline{\Omega})$ we have

$$S(\rho, x, t, u) \leq S(\rho, x, t, v); \tag{2.2}$$

2. stability: for all $\rho > 0$ there exists a solution $u^\rho \in L^\infty(\overline{\Omega})$ to (2.1) with a bound independent of ρ;
3. consistency: for all $x \in \overline{\Omega}$ and $\phi \in C_b^\infty(\overline{\Omega})$ (the set of C^∞ bounded functions),

$$\limsup_{\rho \to 0, y \to x, \xi \to 0} S(\rho, y, \phi(y) + \xi, \phi + \xi) \leq G^*(x, \phi(x), D\phi(x)) \tag{2.3}$$

and

$$\liminf_{\rho \to 0, y \to x, \xi \to 0} S(\rho, y, \phi(y) + \xi, \phi + \xi) \geq G_*(x, \phi(x), D\phi(x)); \tag{2.4}$$

4. strong uniqueness principle: if $u \in L^\infty(\overline{\Omega})$ is an u.s.c subsolution of (1.1) and $v \in L^\infty(\overline{\Omega})$ is an l.s.c supersolution of (1.1), then $u \leq v$ on $\overline{\Omega}$.

THEOREM 2.1 (from Barles and Souganidis). *Assuming the monotonicity, consistency, and stability of the scheme* (2.1) *and the strong uniqueness property of the problem* (1.1)*, then the solution* u^ρ *of* (2.1) *converges locally uniformly to the unique continuous viscosity solution of* (1.1).

The stability, (2.2), (2.3), and (2.4) imply that the functions

$$\bar{u} = \limsup_{\rho \to 0, y \to x} u^\rho(y) \quad \text{and} \quad \underline{u} = \liminf_{\rho \to 0, y \to x} u^\rho(y)$$

are defined on $\overline{\Omega}$; they are, respectively, u.s.c. subsolutions and l.s.c. supersolutions of (1.1). By definition, we have $\underline{u} \leq \overline{u}$. The opposite inequality follows from the uniqueness property. Note that if we have only this uniqueness property on Ω, as is the case for Dirichlet boundary conditions, the same argument shows that $\underline{u} = \overline{u}$ on Ω.

2.2. Two numerical schemes. We consider a bounded open domain Ω that is discretized by means of a triangulation $\mathcal{T}_\rho$. The parameter ρ is the maximum, on the elements T of $\mathcal{T}_\rho$, of the radius of the smallest disk containing T.

We consider a scheme for $H(x, u, Du) = 0$ that is defined for any point of the mesh except perhaps for the boundary nodes. It is written as

$$S_H(\rho, x, u^\rho(x), u^\rho) = 0. \tag{2.5}$$

We also consider an approximation of the boundary conditions that is defined for any node of the triangulation on the boundary of Ω,

$$S_F(\rho, x, u^\rho(x), u^\rho) = 0. \tag{2.6}$$

Let $(x,t,p) \mapsto H_b(x,t,p)$ be a Hamiltonian defined at least in a neighborhood of $\partial\Omega \times \mathbb{R} \times \mathbb{R}^N$. It fulfills the same assumptions as H. We also have a numerical scheme S_{H_b} for the Hamiltonian H_b. We define the following scheme for (1.1):

(2.7)
$$0 = S(\rho, x, u^\rho(x), u^\rho) = \begin{cases} S_H(\rho, x, u^\rho(x), u^\rho) & \text{if } x \in \Omega, \\ \max(S_{H_b}(\rho, x, u^\rho(x), u^\rho), S_F(\rho, x, u^\rho(x), u^\rho)) & \text{if } x \in \partial\Omega. \end{cases}$$

Another a priori reasonable scheme could also be

(2.8)
$$0 = S(\rho, x, u^\rho(x), u^\rho) = \begin{cases} S_H(\rho, x, u^\rho(x), u^\rho) & \text{if } x \in \Omega, \\ \min(S_{H_b}(\rho, x, u^\rho(x), u^\rho), S_F(\rho, x, u^\rho(x), u^\rho)) & \text{if } x \in \partial\Omega. \end{cases}$$

The questions are the following: On which conditions can the scheme (2.7) or (2.8) be considered as a good numerical approximation of (1.1)? Can we identify criteria for preferring scheme (2.7) to (2.8)?

Before giving conditions that ensure the convergence of the schemes (2.7) and (2.8), we motivate the "max" condition of (2.7) in the case of a convex Hamiltonian. The justification comes from the dynamical programming principle and is therefore valid for convex Hamiltonians. We could make the same type of justification for the "min" condition of (2.8) for concave Hamiltonians.

Dynamical programming principle. We assume that the Hamiltonian is given by

$$H(x,u,p) = \sup_{v \in V} \left\{ -b(x,v) \,.\, p + \lambda u - f(x,v) \right\},$$

where the space of controls V is compact, and we have standard assumptions on b and f. We also assume $\lambda > 0$. For the Dirichlet condition (1.5), the solution of (1.1) is given by, for any $T > 0$,

$$0 = u(x) - \inf_{v(.)} \left[\int_0^{\min(T,\tau)} f(y_x(t), v(t)) e^{-\lambda t} dt + 1_{\{T<\tau\}} u(y_x(T)) e^{-\lambda T} + 1_{\{T \geq \tau\}} \varphi(y_x(\tau)) e^{-\lambda \tau} \right]. \tag{2.9}$$

As usual, the trajectory $y_x(.)$ satisfies $y_x(0) = x \in \Omega$ and

$$\frac{d}{dt} y_x(t) = b(y_x(t), v(t)) \quad \text{for } t > 0.$$

The exit time τ is

$$\tau = \inf\{t \geq 0, y_x(t) \notin \Omega\}.$$

Now, the set of controls can be split into two parts: the set V_1 for which $T < \tau$, and V_2 for which $T \geq \tau$. Hence,

$$u(x) = \min\left(\inf_{v \in V_1} [\cdots], \inf_{v \in V_2} [\cdots] \right).$$

Let $\vec{n}$ be the interior normal to Ω at $x \in \overline{\Omega}$. Since T is arbitrary, it can be chosen as small as possible. In the limit $T \to 0$, the set V_1 would be the set of controls for which

$b(x,v)\,.\,\vec{n} > 0$, i.e., the control for which the trajectory goes into Ω. The dynamical programming principle $\inf_{v\in V_1}[\cdots] - u(x) = 0$ corresponds to the Hamiltonian

$$H_b(x,t,p) = \sup_{v\in V_1}\{b(x,v)\,.\,p + \lambda t - f(x,v)\}.$$

We also have the relation $H_b \le H$.

The "inf" on V_2 can be approximated, if T is small, by $\varphi(y_x(\tau))$. Since $T \le \tau$ and if we can choose controls for which $T \simeq \tau$, we get

$$\varphi(y_x(\tau)) \simeq \varphi(x)$$

because φ is continuous. Thus, by setting $S_F = u(x) - \varphi(x)$, we see that (2.9) can be approximated by

$$0 = \max(S_{H_b}, S_F),$$

which is want we wanted. We have the following result.

THEOREM 2.2. *Assume that*

1. $H_b \le H$;
2. S_H, S_{H_b}, *and* S_F *are monotone and stable;*
3. *for all* $\phi \in C_b^\infty(\overline{\Omega})$, *we have*

$$\begin{aligned}
&\text{for any } x \in \overline{\Omega},\\
&\lim_{\rho\to 0, y\to x, \xi\to 0} S_H(\rho, y, \varphi(y)+\xi, \varphi+\xi) = H(x,\varphi(x),D\varphi(x)),\\
&\text{for any } x \text{ in a neighborhood of } \partial\Omega,\\
&\lim_{\rho\to 0, y\to x, \xi\to 0} S_{H_b}(\rho, y, \varphi(y)+\xi, \varphi+\xi) = H_b(x,\varphi(x),D\varphi(x)),\\
&\text{for any } x \in \partial\Omega,\\
&\lim_{\rho\to 0, y\to x, \xi\to 0} S_F(\rho, y, \varphi(y)+\xi, \varphi+\xi) = F(x,\varphi(x),D\varphi(x));
\end{aligned}$$

4. *the equation* (1.1) *has a uniqueness principle.*

Then the family u^ρ *defined by* (2.7) *converges locally uniformly to the solution of* (1.1) *in* Ω. *We have the same result for* (2.8), *provided that the condition* 1 *is replaced by* $H \le H_b$.

Proof. We make the proof for the scheme (2.7). The proof for (2.8) is similar.

We first note that, on the boundary,

$$\begin{aligned}
&\limsup_{\rho\to 0, y\to x, \xi\to 0} S(\rho, y, \varphi(y)+\xi, \varphi+\xi)\\
&\qquad = \max\big(H(x,\varphi(x),D\varphi(x)), \max(H_b(x,\varphi(x),D\varphi(x)), F(x,\varphi(x),D\varphi(x)))\big),
\end{aligned}$$

$$\begin{aligned}
&\liminf_{\rho\to 0, y\to x, \xi\to 0} S(\rho, y, \varphi(y)+\xi, \varphi+\xi)\\
&\qquad = \min\big(H(x,\varphi(x),D\varphi(x)), \max(H_b(x,\varphi(x),D\varphi(x)), F(x,\varphi(x),D\varphi(x)))\big),
\end{aligned}$$

while in the interior points,

$$\lim_{\rho\to 0, y\to x\xi\to 0} S(\rho, y, \varphi(y)+\xi, \varphi+\xi) = H(x,\varphi(x),D\varphi(x)). \tag{2.10}$$

Then we proceed as in [4]. We define

$$\overline{u}(x) = \limsup_{y\to x,\rho\to 0} u^\rho(y) \quad \text{and} \quad \underline{u}(x) = \liminf_{y\to x,\rho\to 0} u^\rho(y).$$

They are defined on $\overline{\Omega}$ because u^ρ has bounds independent of ρ. We will show now that the functions $\overline{u}$ and $\underline{u}$ are, respectively, sub- and supersolutions of (1.1). In fact, we show first that if $x_0 \in \partial\Omega$ is a local minimum of $\underline{u} - \phi$, then

(2.11)
$$\max\big(H(x_0, \underline{u}(x_0), D\varphi(x_0)), \max(H_b(x_0, \underline{u}(x_0), D\varphi(x_0)), F(x_0, \underline{u}(x_0), D\varphi(x_0)))\big) \geq 0,$$

while if $x_0 \in \partial\Omega$ is a local maximum of $\overline{u} - \phi$ for some $\phi \in C^b_\infty(\overline{\Omega})$, then

(2.12)
$$\min\big(H(x_0, \overline{u}(x_0), D\varphi(x_0)), \max(H_b(x_0, \underline{u}(x_0), D\varphi(x_0)), F(x_0, \overline{u}(x_0), D\varphi(x_0)))\big) \leq 0.$$

To show (2.11), we repeat Barles and Souganidis's arguments. Equation (2.12) is obtained in the same way. We may assume that x_0 is a strict minimum, $\underline{u}(x_0) = \phi(x_0)$, and $\phi \leq 2\inf_\rho ||u^\rho||_\infty$ outside of $B(x_0, r)$, where r is such that

$$\underline{u}(x) - \phi(x) \geq \underline{u}(x_0) - \phi(x_0) = 0 \quad \text{in } B(x_0, r).$$

There exist sequences ρ_n and $y_n \in \overline{\Omega}$ such that $n \to +\infty$, $\rho_n \to 0$, $y_n \to x_0$, $u^{\rho_n}(y_n) \to \underline{u}(x_0)$, and y_n is a global minimum of $u^{\rho_n} - \phi$. We denote by ξ_n the quantity $u^{\rho_n}(y_n) - \phi(y_n)$. We have $\xi_n \to 0$ and $u^{\rho_n}(y) \geq \phi(y) + \xi_n$ in $B(x_0, r)$. Since S is monotone, we get

$$0 \leq \limsup_n S(\rho_n, y_n, \phi(y_n) + \xi_n, \phi + \xi_n) \leq \limsup_{\rho\to 0, y\to x_0, \xi\to 0} S(\rho, y, \varphi(y) + \xi, \varphi + \xi)$$

$$= \max(H(x_0, \varphi(x_0), D\varphi(x_0)), \max(H_b(x_0, \varphi(x_0), D\varphi(x_0)), F(x, \varphi(x_0), D\varphi(x_0)))).$$

If $x_0 \in \Omega$ is a local maximum (resp., minimum) of $\overline{u} - \phi$ (resp., $\underline{u} - \phi$), we use (2.10) and the same arguments as above to get

$$H(x_0, \overline{u}(x_0), D\phi(x_0)) \leq 0 \qquad (\text{resp., } H(x_0, \underline{u}(x_0), D\phi(x_0)) \geq 0). \tag{2.13}$$

Now we have to check that the condition (2.12) (resp., (2.11)) implies the supersolution (resp., subsolution) condition.

- *Inequality* (2.12). If $F(x_0, \underline{u}(x_0), D\phi(x_0)) \leq 0$, there is nothing to prove. We assume $F(x_0, \underline{u}(x_0), D\phi(x_0)) > 0$. We have either

  $$H(x_0, \underline{u}(x_0), D\varphi(x_0)) \leq 0 \tag{2.14}$$

  or

  $$\max(H_b(x_0, \underline{u}(x_0), D\phi(x_0)), F(x_0, \underline{u}(x_0), D\phi(x_0))) \leq 0.$$

  In the second case, we necessarily have (2.14), and in both cases the inequality holds.

- *Inequality* (2.11). If $F(x_0, \overline{u}(x_0), D\phi(x_0)) \geq 0$, there is nothing to prove. If we assume $F(x_0, \overline{u}(x_0), D\phi(x_0)) < 0$, then we must have either $H(x_0, \overline{u}(x_0), D\phi(x_0)) \geq 0$ or

$$\max(H_b(x_0, \overline{u}(x_0), D\phi(x_0)), F(x_0, \overline{u}(x_0), D\phi(x_0))) \geq 0.$$

  Since $F < 0$, this inequality implies $H_b \geq 0$, so that

$$H(x_0, \overline{u}(x_0), D\phi(x_0)) \geq H_b(x_0, \overline{u}(x_0), D\phi(x_0)) \geq 0.$$

  Thus, in both cases, we get $H(x_0, \overline{u}(x_0), D\phi(x_0)) \geq 0$, which is what we wanted.

This shows that $\underline{u}$ is a supersolution and $\overline{u}$ is a subsolution of (1.1). The strong uniqueness principle enables us to conclude. □

In the following section, we explain the role of H_b and give some examples for (2.7). These examples can easily be extended to (2.8). In section 4.1, we provide some simple criteria on H for choosing between (2.7) and (2.8).

3. Some examples. In [9, 1], two classes of numerical Hamiltonian were considered, Godunov and Lax–Friedrichs Hamiltonians. Here, we recall the main results of [1] because they can be applied to a more general setting than those of [9] from which they are inspired. In both cases, only the case of the domain $\mathbb{R}^N$ has been studied, i.e., in the present setting, the case of *interior* nodes.

In order to discretize the problem

$$\begin{cases} u_t + H(Du) = 0, \\ u(x,0) = u_0(x) \end{cases}$$

for $x \in \mathbb{R}^N$ and $t > 0$, where u_0 is Lipschitz continuous, we have considered the scheme

$$\begin{aligned} &u_i^0 = u_0(x_i), \\ &u_i^{n+1} = u_i^n - \Delta t \mathcal{H}_\rho(D_{T_1} u^n, \dots, D_{T_{k_i}} u^n). \end{aligned} \tag{3.1}$$

In (3.1), u^n represents the piecewise linear interpolant of (u_j^n), the set $\{T_1, \dots, T_{k_i}\}$ is the set of triangles that contain x_i, and $D_T u^n$ represents the (constant) gradient of u^n in the triangle T. The parameter ρ describes the local geometry of the mesh. In the examples to come, we specify this parameter; see Remark 1. For any $R > 0$, let us introduce the set $\mathcal{C}_R$ of continuous piecewise linear functions defined by

$$\mathcal{C}_R = \{u \text{ continuous piecewise linear s.t. } ||D_T u|| \leq R \text{ for any triangle } T\}. \tag{3.2}$$

We have to define the numerical Hamiltonians $(p_1, \dots, p_k) \mapsto \mathcal{H}_\rho(p_1, \dots, p_{k_i})$. They have been designed to have the following properties:

1. consistency: $\mathcal{H}_\rho(p, \dots, p) = H(p)$,
2. monotonicity: there exists Δt_R such that for all $\Delta t \leq \Delta t_R$, if $u^n, v^n \in \mathcal{C}_R$ and if $u_i^n \leq v_i^n$ for all i, then $u_i^{n+1} \leq v_i^{n+1}$,
3. intrinsicness: the definition of $\mathcal{H}_\rho$ does not depend on the geometrical description of u^n. For any vertex x_i, for any triangle T such that x_i is a vertex of T, if T is split into two triangles T_1 and T_2 for which x_i is still a vertex, then the value of the numerical Hamiltonian is not modified; see Figure 1.

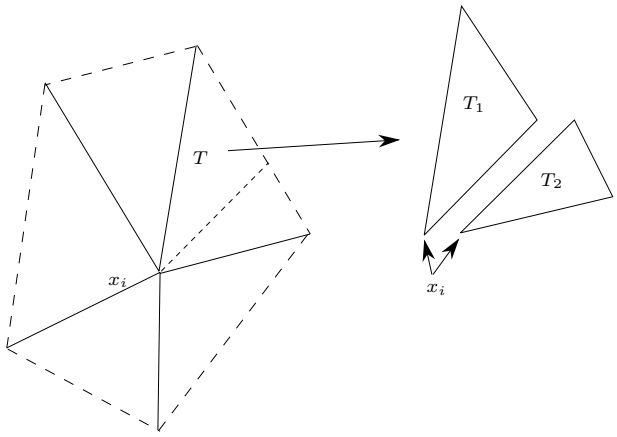

FIG. 1. *Geometrical elements for the intrinsic property: the numerical Hamiltonian is not modified if the triangle T is split into T_1 and T_2 and the value of u at the new vertex is evaluated by linear interpolation.*

We also assume that $\mathcal{H}_\rho$ is *uniformly* continuous in the p and ρ variables. Of course, the number of arguments changes from one mesh point to the other, but if the mesh is regular, the number of neighbors is bounded above, and, thanks to the "intrinsicness" property, we can think of $\mathcal{H}_\rho$ as the same function everywhere. Assuming these properties, it is possible to show the convergence of the scheme (3.1) and to give an error estimate [8, 1].

Notation. In what follows, when we consider numerical schemes that can be put in the form (3.1), sometimes the $D_{T_l}u^n$'s are rewritten in terms of u_i^n and the values of u^n for the neighboring nodes of x_i. For the sake of convenience, we denote the set of the neighbors of x_i (excluding x_i) by $\mathcal{N}_i$, and we rewrite the scheme as

$$u_i^{n+1} = G_\rho(u_i^n, \{u_j^n, j \in \mathcal{N}_i\}; \Delta t). \tag{3.3}$$

More generally, when the Hamiltonian is of the form $H(x, u(x), Du(x))$, the scheme is sometimes rewritten as

$$u_i^{n+1} = G_\rho(x_i, u_i^n, \{u_j^n, j \in \mathcal{N}_i\}; \Delta t) = u_i^n - \Delta t \mathcal{H}_\rho\left(x_i, u_i^n, \{u_j^n, j \in \mathcal{N}_i\}\right). \tag{3.4}$$

In the G-function, $G_\rho(x, t, \{t_l, l \in \mathcal{N}\}; \Delta t)$, t is similar to $u^\rho(x)$, and the variables t, $\{t_l, l \in \mathcal{N}\}$, provide a description of u^ρ in a neighborhood of x_i.

When we are interested in steady problems, the scheme, in the most general case considered in the paper, is

$$\mathcal{H}_\rho(x_i, u_i^n, \{u_j^n, j \in \mathcal{N}_i\}) = 0. \tag{3.5}$$

Similar definitions are also considered for implicit schemes.

In the case of schemes (3.3) and (3.4), the monotonicity condition is equivalent to the following property of G_ρ: $(x, t, \{t_l, l \in \mathcal{N}_i\}) \mapsto G_\rho(x, t, \{t_l, l \in \mathcal{N}_i\}; \Delta t)$. For any fixed grid point $x = x_i$, G should be increasing in t and $\{t_l, l \in \mathcal{N}_i\}$. In practice, the numerical Hamiltonian $\mathcal{H}_\rho$ is an increasing function of $\{t_l, l \in \mathcal{N}_i\}$ and decreasing in t, so that the monotonicity condition for the explicit scheme is true, provided that a CFL-type condition on the time step holds. In the case of schemes (3.5), the monotonicity condition stated in Theorem 2.1 is less restrictive than for unsteady problems: $\mathcal{H}_\rho$ is decreasing with respect to t and increasing with respect to t_l.

Two types of Hamiltonians have been constructed so far, and for the sake of simplicity we describe them in the simplest case. The general case can be treated by "freezing" the x and $u(x)$ variables. They all satisfy the following "translation invariance" property, which mimics the facts that the t-arguments are used to approximate a gradient:

$$\forall x, t, t_l,\, C \in \mathbb{R},\quad G_\rho(x, t + C, \{t_l + C, l \in \mathcal{N}_i\}; \Delta t) = G_\rho(x, t, \{t_l, l \in \mathcal{N}_i\}; \Delta t). \tag{3.6}$$

Godunov Hamiltonians. If $H = H_1 + H_2$, where H_1 (resp., H_2) is convex (resp., concave),[1] then we set

$$\mathcal{H}^G_\rho(p_1, \dots, p_{k_i}) = \inf_{q\in\mathbb{R}^2} \max_{0\le l\le k_i} \sup_{y\in -\Omega_l + q} \left[(p_i \mid y - q) - H_1^*(y) - H_2^*(q)\right], \tag{3.7}$$

where Ω_l, $l = 1, \dots, k_1$, are the angular sectors defined by the triangles $T_1, \dots, T_{k_i}$ at node x_i; H_1^*, for any l, $-\Omega_l$ is the symmetric of Ω_l with respect to x_i; and H_2^* are the Legendre transforms of H_1 and H_2. We have denoted by $(x \mid y)$ the dot product of x and y.

If h is the smallest radius of the circles of center x_i contained in $\cup_{i=1}^{k_i} T_i$, and if L_1 and L_2 are Lipschitz constants for H_1 and H_2, then the scheme is monotone, provided that the time step satisfies

$$\frac{\Delta t}{h}(L_1 + L_2) \le \frac{1}{2}.$$

The numerical Hamiltonian (3.7) is obtained by saying that $H_1 + H_2$ is bounded below by the convex functions $H_q(p) = H_1(p) - (p \mid q) + H_2^*(q)$. Another monotone Hamiltonian can also be obtained, as in [1], by saying that $H_1 + H_2$ is bounded above by the concave functions $H_q(p) = H_2(q) + (p \mid q) - H_1^*(p)$.

Lax–Friedrichs Hamiltonians. Here we set

$$\mathcal{H}^{LF}_\rho(p_1, \dots, p_{k_i}) = H(\bar{U}) - \frac{\epsilon}{h} \oint_{C_h} [u(x) - u(x_i)] dl,$$

where C_h (resp., D_h) is a circle (resp., disk) of center x_i and radius h,

$$\widehat{U} = \frac{\int_{D_h} Du\, dxdy}{\pi h^2},$$

and ϵ is larger than any Lipschitz constant of H divided by 2π.

Remark 1. For the Godunov and Lax–Friedrichs Hamiltonians, and at a mesh node x, the ρ parameter is the set of unit vectors defining the edges of the triangles at this node and the angles (at node x) of the triangles; see Figure 2.

3.1. Godunov boundary Hamiltonians for convex Hamiltonians. We look for a Hamiltonian $\mathcal{H}^b_\rho$ of the form

$$\mathcal{H}^b_\rho(p_1, \dots, p_k) = \max_{0\le l\le k_i} \sup_{z\in -\Omega_l} \{(p_l \mid z) - H_b^*(z)\},$$

where the p_i's are the local gradients of a piecewise linear continuous function defined on $\overline{\Omega}$ and the Ω_l's are the angular sectors as before. We need that

$$\mathcal{H}^b_\rho(p, \dots, p) = H_b(p) \le H(p).$$

[1] In the case of a Cartesian mesh, this assumption can be relaxed as shown in [9].

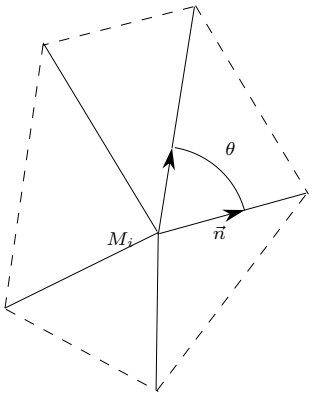

FIG. 2. *A description of* ρ.

If we assume that H_b is convex, this inequality implies $H_b^* \geq H^*$; the most natural choice is to take

$$\begin{cases} H_b^*(q) = H^*(q) & \text{if } q \in \cup_{j=1}^{k_i} \Omega_j, \\ H_b^*(q) = +\infty & \text{otherwise,} \end{cases} \tag{3.8}$$

but any convex Hamiltonian K such that $K^* \geq H_b^*$, which domain is included in $\cup_{j=1}^{k_i} \Omega_j$, would also be a solution. The monotonicity condition is automatically satisfied, thanks to the Hopf formula. In the case of an unsteady problem, the same CFL condition is valid; i.e., if L is a Lipschitz constant of H, the time step satisfies

$$\frac{\Delta t}{h} L \leq \frac{1}{2},$$

because the Lipschitz constant of H_b is at most that of H. If L is a Lipschitz constant of H, $H^*(p)$ may be finite only if p belongs to the ball $B(0, L)$ of center 0 and radius L. Since H_b^* is finite when H is finite, a Lipschitz constant of H is a Lipschitz constant for H_b.

Note that the Hamiltonian (3.8) is the largest possible choice and is the one suggested by the analysis from the dynamical programming principle. It can be interpreted by saying that we take into account all the outgoing rays.

3.2. Godunov boundary Hamiltonians for concave Hamiltonians. The analysis via the dynamical programming principle suggests choosing the boundary condition (2.8). We define H_b by (3.8), where the $+\infty$ condition is replaced by $-\infty$.

3.3. Lax–Friedrichs boundary Hamiltonians for convex Hamiltonians. Here, we are looking for Hamiltonians of the type

$$\mathcal{H}_\rho^b(p_1, \ldots, p_k) = K(\bar{U}) - \frac{\epsilon_b}{h} \oint_{C_h} [u(x) - u(x_i)] dl,$$

where K is unknown, as well as the numerical dissipation ϵ_b. The average state is once more defined by

$$\bar{U} = \frac{\int_{D_h \cap \Omega} Du \, dxdy}{|D_h \cap \Omega|}.$$

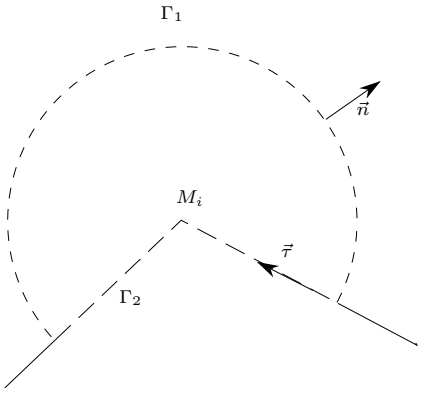

FIG. 3. *Definition of* Γ_1 *and* Γ_2.

The monotonicity condition is satisfied, provided that, L_b being a Lipschitz constant of K,

$$\epsilon_b \geq \frac{L_b\, h}{|D_h \cap \Omega)|}.$$

The area $\partial(D_h \cap \Omega)$ is $\theta\, h$, where θ is the angle of $D_h \cap \Omega$ at x_i. This can be seen by using the same arguments as in [1].

We denote by Γ_1 the part of $\partial(D_h \cap \Omega)$ which is inside Ω, and by Γ_2 the boundary part; see Figure 3. To determine K, we consider the consistency condition. It is easy to see that

$$H_b(p) \equiv \mathcal{H}^b_\rho(p, \dots, p) = K(p) - \frac{\epsilon_b}{h}\left(p \middle| \left\{ \int_{\Gamma_1} \vec{n} dl - \int_{\Gamma_2} \vec{\tau} dl \right\}\right),$$

where $\vec{n}$ is the outward unit normal to Γ_1 and $\vec{\tau}$ is the unit tangent vector to Γ_2. The vector

$$\vec{N} = -\frac{1}{h}\left(\int_{\Gamma_1} \vec{n} dl - \int_{\Gamma_2} \vec{\tau} dl \right)$$

enters into Ω if $\partial\Omega$ is regular enough.

The convergence property of Theorem 2.2 is satisfied if $H_b \leq H$. When H_b is assumed to be convex, this condition is equivalent to asking for K to be convex and

$$\left(K + \epsilon_b \left(\vec{N} \mid \ . \ \right)\right)^* (q) \geq H^*(q) \quad \forall q \in \mathbb{R}^2.$$

The Legendre transform of $x \mapsto K(x) + \epsilon_b(\vec{N}|x)$ is

$$q \mapsto K^*(q + \epsilon_b \vec{N}),$$

and consequently K^* is defined by the relation

$$K^*(q) \geq H^*(q - \epsilon_b \vec{N}). \tag{3.9}$$

Let us call $\mathrm{Dom}(H^*)$ (resp., $\mathrm{Dom}(H_b)$) the subset of $\mathbb{R}^2$ for which $H^*(q)$ (resp., $(H^b)^*$) is finite. If L is a Lipschitz constant of H, $\mathrm{Dom}(H^*) \subset B(L)$. A similar result holds

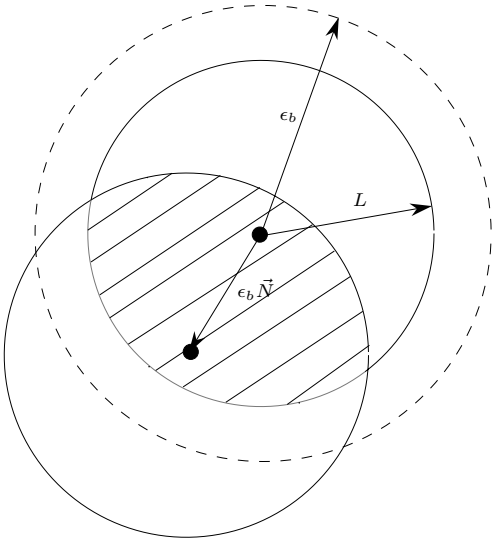

FIG. 4. *Geometrical representation of the conditions.*

for K. These sets are convex. There is a solution to the problem (different from $K = -\infty$) if and only if we can find ϵ_B such that

$$\begin{aligned} &(\mathrm{Dom}(H) - \epsilon_b\vec{N}) \cap \mathrm{Dom}(H) \neq \emptyset, \\ &(\mathrm{Dom}(H) - \epsilon_b\vec{N}) \cap B(\epsilon_b) \neq \emptyset. \end{aligned} \tag{3.10}$$

See Figure 4 for a representation of these conditions.

In some cases, there is *no* solution at all. The simplest counterexample is given by

$$H(x) = (\vec{a} \mid x)$$

with $\vec{a} \neq 0$. In this case, $\mathrm{Dom}(H) = \{\vec{a}\}$. The first condition implies $\epsilon_b = 0$ (thus $||\vec{a}|| = 0$); the second one gives $\vec{a} = 0$.

In some cases, there are solutions. An example is given by any Hamiltonian for which $\min H > -\infty$: since $0 \in \mathrm{Dom}(H)$, we can set $\epsilon_b = 0$ and $K \equiv \min H$. Another example is provided by $H(x) = ||x||$. Here, we can choose any $\epsilon_b \in [0, \frac{1}{2||\vec{N}||}]$.

3.4. Other choices. In sections 3.1 and 3.3, a very obvious choice would be $H_b \equiv -\infty$. This choice enables us to satisfy our convergence conditions. In fact we have

$$\begin{aligned} &\min(H, \max(-\infty, F)) = \min(H, F), \\ &\max(H, \max(-\infty, F)) = \max(H, F), \end{aligned}$$

so that the viscosity inequalities are obviously satisfied. This reduces to strongly imposing the boundary conditions. However, this is not be the best choice, since a numerical boundary layer may be generated, especially in the case of Dirichlet boundary conditions. The scheme converges, but very slowly, as can be seen by numerical experiments; see section 5. Moreover, the results of this paper have been formally extended to more general cases, particularly the case of discontinuous Dirichlet conditions. In this particular case, the choice $H_b = -\infty$ may prevent convergence, whereas the Godunov or Lax Friedrichs boundary Hamiltonian seems to ensure convergence.

It now becomes clear that some selection procedures must be established. We will provide some, in special cases.

4. Some selection criteria. In this section, we discuss the problem of finding suitable boundary Hamiltonians and the question of selecting between the min and max conditions. These two questions are related, but the most difficult one is to find a "good" boundary Hamiltonian. If no care is taken, the numerical solution may develop a boundary layer structure, especially in the case of Dirichlet conditions; i.e., the gradient of the numerical solution may become unbounded when the mesh size tends to zero. If Theorem 2.2 provides some necessary conditions for convergence, this is not acceptable in general because practical calculations are done with finite but nonvanishing mesh sizes.

This situation is very similar to the technical difficulties encountered in the analysis of the boundary problem in the continuous case; see [4]. To explain this point, let us consider a simple one dimensional example.

If, for example, we think of a numerical scheme for

$$\begin{cases} |u'(x)| = 1, & x \in]0,1[, \\ u(0) = 0, & u(1) = 2, \end{cases}$$

where the boundary conditions are strongly imposed as being modeled by

$$\begin{cases} |u'(x)| - \epsilon u_{xx} = 1, & x \in]0,1[, \\ u(0) = 0, & u(1) = 2, \end{cases} \tag{4.1}$$

the solution should look like

$$u_\epsilon(x) = x + \frac{\exp\left(\frac{x-1}{\epsilon}\right) - \exp\left(-\frac{1}{\epsilon}\right)}{1 - \exp\left(-\frac{1}{\epsilon}\right)},$$

and hence a boundary layer exists: the derivative of u is not bounded at $x = 1$ when $\epsilon \to 0$. Its thickness tends to 0 as $\epsilon \to 0$.

This simple example is quite generic from the numerical point of view. Assume that the numerical solution u^ρ converges in the neighborhood of the boundary to a regular solution u. Then, up to second order truncation errors, the numerical Hamiltonian behaves like

$$H(p_1, \dots, p_{k_i}) \simeq H(Du) - \epsilon(\rho) D^2 u,$$

where D^2u represents some elliptic operator and $\epsilon(\rho) \to 0$ as the mesh size tends to zero. In [8], some numerical schemes are constructed by directly using this idea. Because of that, if one sets the boundary condition strongly on $\partial\Omega$, as in the example (4.1), a boundary layer must exist in the vicinity of $\partial\Omega$. Its thickness tends to 0 as $\epsilon \to 0$. Its thickness also tends to 0 as $\epsilon(\rho) \to 0$.

4.1. Choosing between the "min" and "max" conditions for Dirichlet boundary conditions. In some situations, the choice can be motivated by some a priori knowledge of the behavior of the exact solution. For example, if one makes the following assumption—there exists $R \in]0, +\infty[$ such that

$$\lim_{\lambda \to +\infty} H(x, u, p - \lambda \vec{n}) = +\infty$$

uniformly on x in a neighborhood of $\partial\Omega$, $-R \le u \le R$ and p bounded[2]—then one can prove that if φ is continuous and u is the solution of

$$\begin{array}{ll} H(x,u(x),Du(x))=0, & x\in\Omega,\\ u(x)=\varphi(x), & x\in\partial\Omega, \end{array}$$

then $u(x)\le\varphi(x)$ on $\partial\Omega$ (see [4]). The boundary condition (2.7) implies that $u\le\phi$ at the discrete level, while (2.8) implies the opposite inequality. Hence, when the above assumption is true, the boundary condition (2.7) is the natural one to consider. This situation is encountered for nonbounded convex Hamiltonians.

When we have

$$\lim_{\lambda\to+\infty} H(x,u,p-\lambda\vec{n})=-\infty,$$

the boundary condition (2.8) is the natural one to consider. This situation is encountered for nonbounded concave Hamiltonians.

4.2. The case of coercive Hamiltonians and boundary conditions (2.7). We are not able to provide an error bound between the numerical and the exact solutions. However, when the Hamiltonians H and H_b are coercive, we can show that no numerical boundary layer can appear; i.e., the gradient of the numerical solution is bounded when the mesh size tends to zero.

We say that H is coercive if

$$H(x,u,p)\to+\infty \quad \text{when } ||p||\to+\infty$$

uniformly for $x\in\Omega$, $u\in[-R,R]$, $R\in]0,+\infty[$. We say that the boundary Hamiltonian is coercive if

$$H_b(x,u,p)\to+\infty \quad \text{when } ||p||\to+\infty \text{ and } (p\mid\vec{n})\ge 0$$

uniformly for $x\in\partial\Omega$, $u\in[-R,R]$ for all $R\in[0,+\infty[$. Here $\vec{n}$ is the inward unit vector at point $x\in\partial\Omega$. We have implicitly assumed that $\partial\Omega$ is C^1. In what follows, we consider the Dirichlet problem

(4.2)
$$\begin{cases} \mathcal{H}_\rho(x_i,u_i,D_{T_1}u,\dots,D_{T_{i_k}}u)=0, & x_i \text{ interior node and } i_l\in\mathcal{N}_i,\\ \max(\mathcal{H}_\rho(x_i,u_i,D_{T_1}u,\dots,D_{T_{i_k}}u),u_i-\varphi(x_i))=0, & x_i \text{ boundary node and } i_l\in\mathcal{N}_i \end{cases}$$

but our results clearly extend to the more general case considered in this paper.

PROPOSITION 4.1. *Let $\mathcal{H}_\rho$ and $\mathcal{H}^b_\rho$ be monotone Hamiltonians consistent with H and H_b. Assume that $\mathcal{H}_\rho$ and $\mathcal{H}^b_\rho$ also satisfy* (3.6)*, and that H and H_b are continuous, convex, and coercive. Assume also that the mesh is regular. Then the scheme* (2.7) *is convergent and the maximum over the triangles T of the norm of the numerical solution, when $h\to 0$ remains bounded.*

The boundary of $\Omega_h=\cup_{T\in\mathcal{T}_h}T$ is denoted by Γ_h.

Proof. The convergence is a consequence of Theorem 2.2. The uniform boundedness of the gradients is a consequence of the following lemma. ∎

LEMMA 4.2. *If H, $\mathcal{H}_\rho$, $\mathcal{H}^b_\rho$, and the mesh satisfy the assumptions of Proposition* 4.1*, and if u is a subsolution of* (4.2)*, then there exists C independent of h such that for any two mesh points M_i, M_j we have*

$$|u_i-u_j|\le CM_iM_j.$$

[2] $\vec{n}$ is the inward unit normal to $\partial\Omega$.

Proof. For the sake of simplicity, we assume that H and H_b depend only on the p variable.

Let $K > 0$ and x_i be a mesh point. For now we let K be free. Since Ω_h has a finite number of points, there exists M', a mesh point such that $u_l - KM_lM_i$ is maximum at M':

$$u_l - KM_lM_i \leq u_{M'} - KM'M_i.$$

This indicates that $v_l = (u(x') - K\,||x' - x_i||) + K\,||x_l - x_i||$ is greater that u, with an equality at node x'. Hence, using the same techniques as in Appendix A, if x' is an interior node,

$$0 \geq \mathcal{H}_\rho(u) \geq \mathcal{H}_\rho(K\,||x - x_i||), \tag{4.3}$$

where we have written $\mathcal{H}_\rho(u)$ instead of $\mathcal{H}_\rho(D_{T_{i_1}}u, \ldots, D_{T_{i_k}}u)$, for short. Similarly, since $\max(\mathcal{H}^b_\rho(u), u - \varphi) \leq 0$, we have $\mathcal{H}^b_\rho(u)$, and by the monotonicity of $\mathcal{H}^b_\rho$, we get

$$0 \geq \mathcal{H}_\rho(K\,||x - x_i||) \tag{4.4}$$

at x' if it is on the boundary. Assume that $x' \neq x_i$. We show that if K is large enough, we have a contradiction. We can assume that $x_i = 0$ so that we have to deal with the piecewise interpolant $\pi_h||x||$ of the convex function $x \mapsto ||x||$. Note that $0 = x_i$ does not lie in the interior of any triangle. A simple consequence of the Taylor formula [7] shows that there exists $C' > 0$ such that if the mesh is regular,

$$\left|\left| D_T\pi_h|x| - \frac{x_G}{||x_G||} \right|\right| \leq C_1 h,$$

where x_G is the gravity center of T.

Since H is regular, there exist $C_2 > 0$ such that

$$\left| \mathcal{H}_\rho(\pi_h||x||) - \mathcal{H}_\rho\left(K\frac{x_{G_1}}{||x_{G_1}||}, \ldots, K\frac{x_{G_k}}{||x_{G_k}||} \right) \right| \leq C_2 h.$$

The same inequality is also true for $\mathcal{H}^b_\rho$. Since the scheme is consistent with uniformly continuous numerical Hamiltonians, and because $O = x_i$ does not belong to the interior of the molecule associated with x', we can replace $\mathcal{H}_\rho(K\frac{x_{G_1}}{||x_{G_1}||}, \ldots, K\frac{x_{G_k}}{||x_{G_k}||})$ by $H(K\ \frac{x'}{||x'||})$ up to an $O(h)$ term. The same is true for $\mathcal{H}^b_\rho$. Hence we get that $H(K\ \frac{x'}{||x'||}) \leq O(h)$, which is impossible if K is large enough. This shows that if $K = C + 1$, where C is chosen so that

$$H(C\,p) < 0 \text{ with } ||p|| = 1 \quad \text{and} \quad H_b(C\,p) < 0 \text{ with } ||p|| = 1 \text{ and } (p \mid \vec{n}) < 0,$$

we have that $x' = x_i$, and then

$$u_l - u_i \leq K||x_l - x_i||$$

when h is small enough. The conclusion holds by symmetry. ∎

An example. We consider the example of a convex Hamiltonian. The boundary Hamiltonian consistent with the Godunov boundary Hamiltonian is

$$H_b(p) = \max_{(y \mid \vec{n}) \leq 0} \left((y \mid p) - H^*(y) \right),$$

where $\vec{n}$ is the inward unit vector. If we assume that H is smooth enough, the optimal ray is $p^* = DH(p)$. A sufficient (and crude) condition to ensure that H_b is coercive if H is coercive is to state that $(p^* \mid \vec{n}) \leq 0$, because in this case $H_b(p) = H(p)$. To obtain this sufficient condition, it is enough to say that

$$\lambda \in \mathbb{R}^+ \mapsto H(p + \lambda \vec{n})$$

is monotone increasing. This has to be connected to the conditions of section 4.1. An example where $(p^* \mid \vec{n}) \leq 0$ is given by the eikonal Hamiltonian because $p^* = \frac{p}{||p||}$.

4.3. Extension to nonconvex Hamiltonians. Let us consider a problem where $H = H_1 + H_2$, with H_1 convex and H_2 concave. Following (3.7), a natural boundary Hamiltonian is also

$$\mathcal{H}^b_\rho(p_1, \ldots, p_{k_i}) = \inf_{q \in \mathbb{R}^2} \max_{0 \leq l \leq k_i} \sup_{y \in -\Omega_l + q} \left[(p_i \mid y - q) - H_1^*(y) - H_2^*(q) \right].$$

Since $\cup_l \Omega_l$ is a strict subset of $\mathbb{R}^2$, we have

$$H^b(p) \equiv \inf_{q \in \mathbb{R}^2} \sup_{(y \mid \vec{n}) \geq 0} \left[(p \mid y - q) - H_1^*(y) - H_2^*(q) \right] \leq H(p),$$

and the conditions of Theorem 2.2 are satisfied.

If the family $\{H_1(p) - (p \mid q)\}_{q \in \mathbb{R}^2}$ is uniformly coercive, then the numerical solution develops no numerical layer; this is a simple consequence of Proposition 4.1.

5. Applications.

5.1. Some numerical tests. We have not been able to get error estimates for the schemes presented above. Even in the case of the crudest approximations of the boundary condition, i.e., by taking $H_b = -\infty$, we can show the convergence of the numerical solution. However, we have shown in a special case that no numerical boundary layer exists even for Dirichlet conditions when the Hamiltonians are coercive.

The purpose of this paragraph is to illustrate the various phenomena that we have encountered, for Dirichlet and Neuman conditions. In each case, the strong boundary conditions are obtained with $H_b = -\infty$, and the weak ones with H_b being the Godunov Hamiltonian. In sections 5.1.1 and 5.1.2, the interior Hamiltonian is the Lax–Friedrichs one. In section 5.2, it is the Godunov Hamiltonian. Other experiments with the Lax–Friedrichs condition have been done, but they are not reported here. They provide the same results. We also show the behavior of the schemes on a problem with nonconvex Hamiltonians and Dirichlet conditions; this is the subject of section 5.1.3.

5.1.1. Dirichlet conditions. The domain Ω is limited by two "concentric" circles of radius 0.5 and 1. It is discretized by a finite element–type mesh, but this is not essential. The problems are

$$\left\{ \begin{array}{ll} ||Du|| = 1 & \text{in } \Omega, \\ u = 0 & \text{for } ||x|| = 0.5, \\ u = C & \text{for } ||x|| = 1. \end{array} \right. \tag{5.1}$$

TABLE 5.1
Boundary condition for the Dirichlet boundary conditions.

Case	1	2	3	4
C	0.5	10	0.25	-11

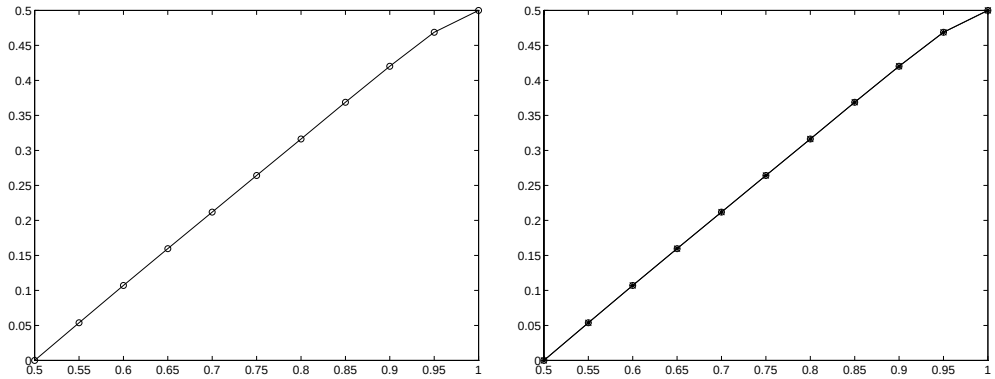

FIG. 5. *Comparison of different implementations of Dirichlet conditions for problem* (5.1) *and Case* 1: (a) *weak conditions,* (b) *comparison of weak* ($\circ$) *and strong* ($*$).

The constant C takes the values displayed in Table 5.1.

The viscosity solution is given as follows:

- Case 1 and 2: $u(x) = ||x|| - 0.5$;
- Case 3: $u(x) = ||x|| - \frac{1}{2}$ if $||x|| \in [\frac{1}{2}, \frac{7}{8}]$ and $u(x) = -||x|| + \frac{5}{4}$ if $||x|| \in [\frac{7}{8}, 1]$;
- Case 4: $u(x) = -||x|| + \frac{1}{2}$.

The difference between these test cases is that for Cases 1 and 3, the boundary conditions on $||x|| = 1$ are enforced strongly, whereas for 2 and 4, they are enforced in the viscosity sense only.

We plot the cross section only in the y-direction and positive abscissa. Two kinds of tests have been done. In the first, we have strongly imposed the boundary conditions; i.e., we have taken $H_b = -\infty$. In the second test, the conditions have been imposed weakly, with the Godunov boundary Hamiltonian.

Comparison of Figures 5, 6, 7, 8 clearly shows that when the boundary condition is *strongly* enforced by the viscosity solution, no special treatment is needed. On the contrary, when it is only weakly enforced, then a special treatment is mandatory, otherwise a boundary layer–type phenomenon is observed.

5.1.2. Neumann conditions. Here, we test the problem

$$\begin{cases} ||Du|| = 1 & \text{in } \Omega, \\ u = 0 & \text{for } ||x|| = 1, \\ \frac{\partial u}{\partial n} = 0 & \text{for } ||x|| = 0.5. \end{cases} \tag{5.2}$$

Its solution is $u(x) = -||x|| + \frac{1}{2}$.

The viscosity solution is given by the solution for Case 1. Once more, the numerical solution is obtained by imposing the boundary conditions either strongly or weakly.

The problem $\frac{\partial u}{\partial n} = g$ is approximated at node A in the following way (see Figure 9). The outward unit normal is approximated as $\vec{n}_A = \overrightarrow{AB}^{\perp} + \overrightarrow{AC}^{\perp}$, which is

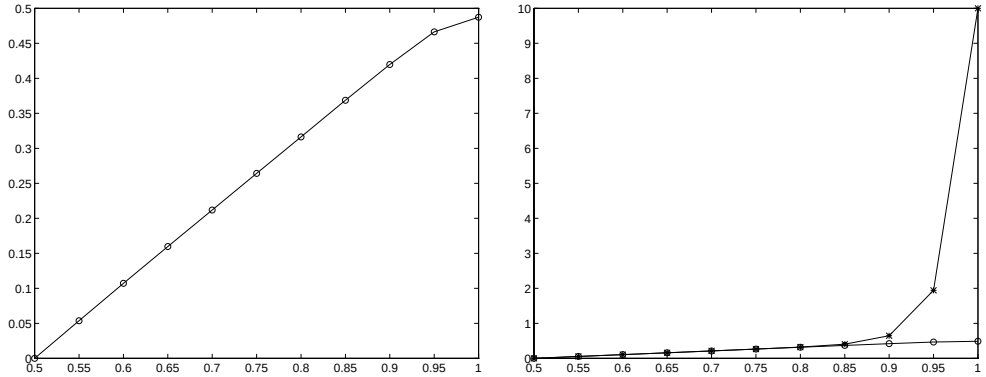

FIG. 6. *Comparison of different implementations of Dirichlet conditions for problem* (5.1) *and Case* 2: (a) *weak conditions,* (b) *comparison of weak* ($\circ$) *and strong* ($*$).

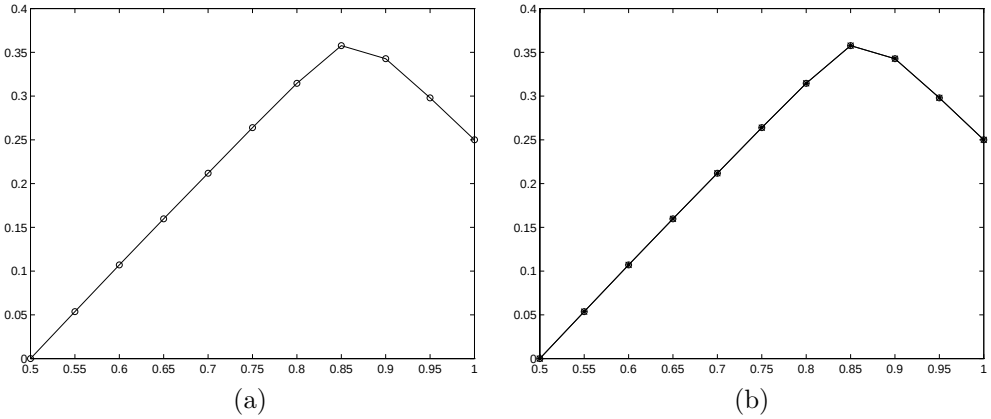

FIG. 7. *Comparison of different implementation of Dirichlet conditions for problem* (5.1) *and Case* 3: (a) *weak conditions,* (b) *comparison of weak* ($\circ$) *and strong* ($*$).

normalized. Here, $\vec{x}^{\perp}$ is the orthogonal vector to $\vec{x}$ such that $(\vec{x}, \vec{x}^{\perp})$ is positive. Then we consider a node D which is on the side of the triangle opposite to D, which is cut by $-\vec{n}_A$. We then set

$$u(A) = ||\overrightarrow{AD}||g(A) + u(C). \tag{5.3}$$

Here, u is the piecewise linear interpolation of the data.

In the strong formulation, we use (5.3) directly. In the weak formulation, we set

$$\max\left(\frac{u_A^{n+1} - u_A^n}{\Delta t} - \mathcal{H}_\rho^b(u^n), \frac{u_A^{n+1} - u_C^{n+1}}{AC} - g(u_A^n)\right) = 0.$$

From Figure 10, it is clear that the weak formulation gives much better results. However, the difference between the two formulations is not as important as for the Dirichlet problem, as expected.

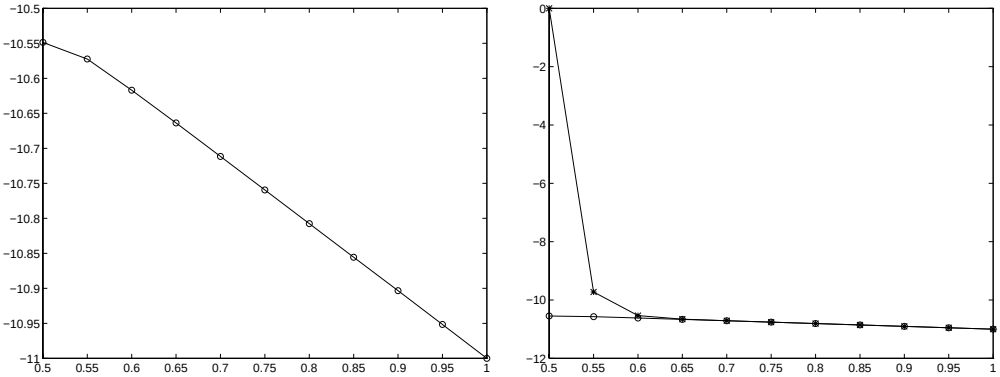

FIG. 8. *Comparison of different implementation of Dirichlet conditions for problem* (5.1) *and Case* 4: (a) *weak conditions,* (b) *comparison of weak* (∘) *and strong* (∗).

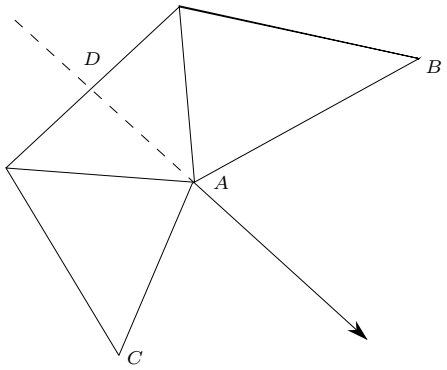

FIG. 9. *Schema for the approximation of the Neuman boundary conditions.*

5.1.3. The case of a nonconvex Hamiltonian and Dirichlet conditions. In general, it is difficult to compute analytically the solution of a first order Hamilton–Jacobi equation, and the situation is even worse when the Hamiltonian is not convex (nor concave), because the analogy with hyperbolic systems becomes looser in general. Hence, it becomes more difficult to judge the quality of numerical results. To overcome this difficulty in a special case, we consider $H(p) = (||p|| - 1)^3$ and the problem

$$\begin{array}{ll} H(Du) = 0 & \text{on } \Omega, \\ u = 0 & \text{on } \Gamma_1, \\ u = 10 & \text{on } \Gamma_2, \end{array} \tag{5.4}$$

where Ω is depicted in Figure 11. Since $t \mapsto t^3$ is monotone increasing, u is a solution of (5.4) if and only if it is a solution of

$$\begin{array}{ll} ||Dv|| - 1 = 0 & \text{on } \Omega, \\ v = 0 & \text{on } \Gamma_1, \\ v = 10 & \text{on } \Gamma_2. \end{array} \tag{5.5}$$

The solution of (5.4) and (5.5) is the distance to Γ_1.

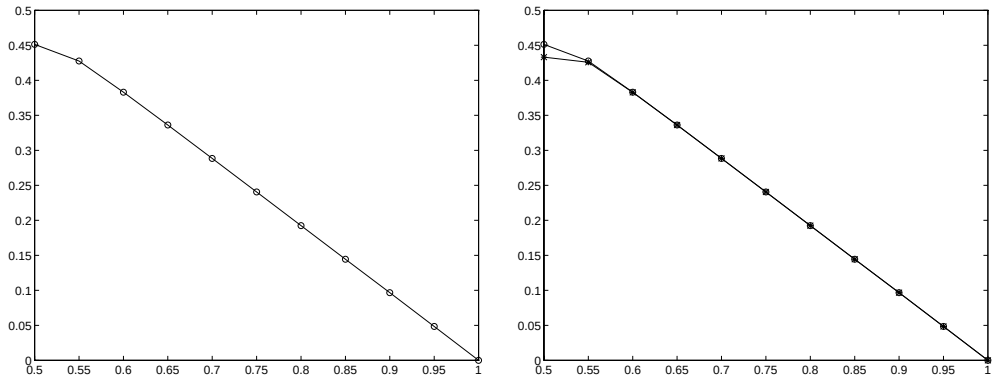

FIG. 10. *Comparison of different implementations of homogeneous Neumann conditions for problem* (5.2): (a) *weak conditions,* (b) *comparison of weak* ($\circ$) *and strong* ($*$).

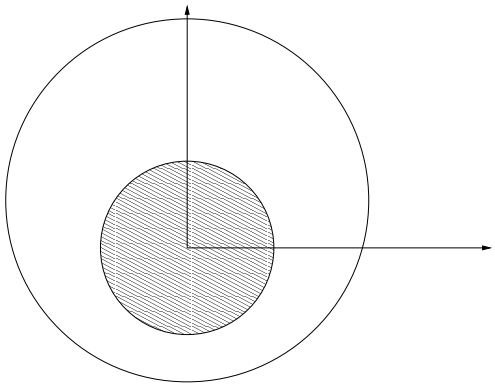

FIG. 11. *Computational domain for problem* (5.4). Γ_1 *is the inner circle of center* $(0,0)$ *and radius* $r=1$, Γ_2 *is the outer circle of center* $(0,0.5)$ *and radius* $r=3$.

In order to discretize (5.4), we write $H = H_1 + H_2$, with $H_1(p) = \max(|p|| - 1, 0)^3$ and $H_2(p) = \min(||p|| - 1, 0)^3$. These functions are respectively convex and concave. The numerical Hamiltonian and the boundary Hamiltonian are the same as in sections 3 and 4.3. The numerical solution is displayed in Figure 12(a). The solution of (5.5) with the Godunov Hamiltonian is provided in Figure 12(b). A close comparison shows that they are (almost) identical.

Another application of the boundary conditions developed in this paper is given by the approximation of the following problem, on the same geometry:

$$\begin{array}{ll} H(Du) = 0 & \text{on } \Omega, \\ u(x,y) = 0, & (x,y) \in \Gamma_1, \\ u(x,y) = 3\cos(2\pi x), & (x,y) \in \Gamma_2. \end{array} \tag{5.6}$$

Since H is nonconvex, it is difficult to know a priori what the value of the solution on the boundary would be. The computed solution is given in Figure 13(a). It can be seen that the solution satisfies the boundary condition strongly on Γ_2 and only weakly on Γ_1 (in contrast to the previous example). Note, however, that the boundary conditions have been numericaly *weakly* imposed on Γ_1 and Γ_2. The solution is also

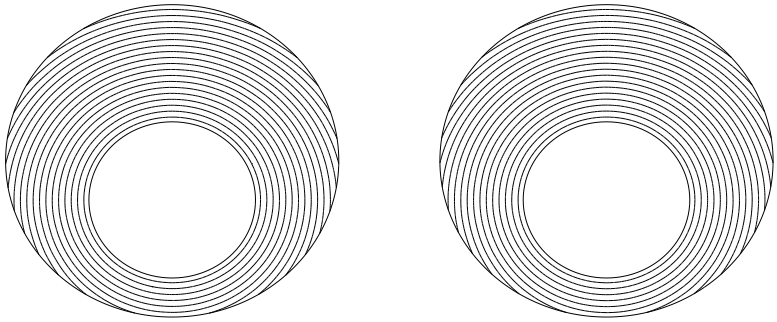

(a) (b)

FIG. 12. (a) *Solution of problem* (5.4), min = 0, max = 1.48. (b) *Solution of problem* (5.10), min = 0, max = 1.504.

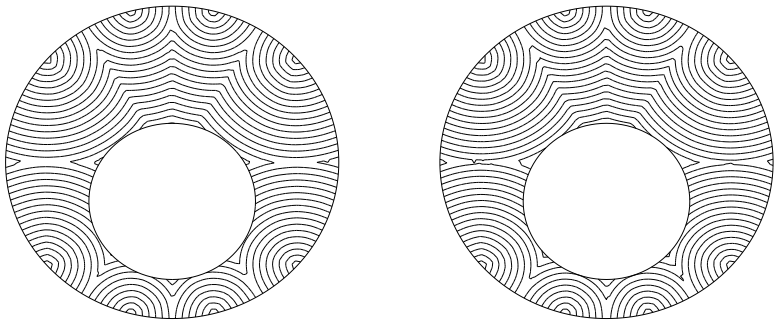

(a) (b)

FIG. 13. (a) *Solution of problem* (5.6), min = −3, max = −1.53. (b) *Solution of problem* (5.7), min = −3, max = −1, 47.

in very good agreement with the one obtained from the discretization of

$$\begin{array}{ll} ||Dv|| - 1 = 0 & \text{on } \Omega, \\ v(x,y) = 0, & (x,y) \in \Gamma_1, \\ v(x,y) = 3\cos(2\pi x), & (x,y) \in \Gamma_2, \end{array} \tag{5.7}$$

which is displayed in Figure 13(b).

5.2. Application to a problem in geophysics. In [6] is developed a technique to compute the multivalued solutions τ of the Eikonal equation with an initial condition

$$\tau(x_S) = 0$$

at the source term x_S. This corresponds to the problem of computing the very high frequency approximation of the wave equation in a possibly inhomogeneous media, when the source term is located at a single point with a Dirac source term. In this case, the solution consists of a wave front that might have a very complex structure.

The solution of this problem is important in geophysics applications; it is the core of an inverse method for reconstructing the index of the media knowing only the arrival times of the wave fronts at the ground.

In Benamou's method [6], we need to be able to solve, in several arbitrary domains Ω containing x_S, the following problem:

$$\begin{cases} ||D\tau|| - n(x) = 0 & \text{in } \Omega, \\ \tau(x_S) = 0, & \\ \tau(x) = +\infty & \text{if } x \in \partial\Omega - \{x_S\}. \end{cases} \tag{5.8}$$

The boundary conditions have to be understood in the viscosity sense. In particular, the second boundary solution corresponds to the Soner boundary condition. The solution to this problem is known,

$$\tau(x) = \inf_{y_x} \left[\int_0^{\min(T,\zeta)} n(y_x(s)) \left| \frac{dy_x}{ds} \right| ds \right], \tag{5.9}$$

where the trajectory y_x starts at x_S for $s = 0$, and ζ is its first exit time, i.e.,

$$\zeta = \inf\{s \geq 0; y_x(s) \notin \overline{\Omega}\}.$$

In other words, we do not take into account the rays that start at x_S and come into Ω.

The idea is to characterize the solution of (5.8) as the steady solution of

$$\begin{cases} u_t + ||Du|| - n(x), & t > 0 \text{ and } x \in \Omega, \\ u(x, t = 0) = 0, & x \in \Omega, \\ u(x_S, t) = 0 & \text{at } x_S \\ u(x, t) = +\infty, & x \in \partial\Omega - \{x_S\}. \end{cases} \tag{5.10}$$

It is clear that neither (5.9) nor (5.10) falls into the framework that we have considered here. The idea is to introduce an approximation of τ_ρ^e, the solution of

$$\begin{cases} ||D\tau|| - 1 = 0 & \text{in } \Omega, \\ \tau(x_S) = 0, & \\ \tau(x) = 0, & x \in \partial\Omega - \{x_S\}, \end{cases} \tag{5.11}$$

given by (5.9) for $n \equiv 1$. We then show that the scheme (5.12) can be rewritten as

$$\begin{cases} \frac{u_i^{n+1} - u_i^n}{\Delta t} + \mathcal{H}_\rho(D_{T_1} u^n, \ldots, D_{T_1} u^n) - n(x_i), & n > 0 \text{ and } x_i \text{ interior point}, \\ u_i^0 = 0 & \text{for all } i, \\ u_{x_S}^n = 0 & \text{for } n \geq 1, \\ u_i^n = \min(u_i^n - \Delta t \mathcal{H}_\rho^b(D_{T_1} u^n, \ldots, D_{T_1} u^n) - n(x_i), K\tau_\rho^e), & n > 0 \text{ and } x_i \neq x_S, \end{cases} \tag{5.12}$$

for K large enough, uniformly in ρ. Once this is shown, we can apply the arguments of (2.2) to conclude. In what follows, we restrict ourselves to the case of the Godunov Hamiltonian.

5.2.1. Finding an elementary supersolution of (5.11) when $n \equiv 1$. Our aim is to find an elementary supersolution of

$$\begin{cases} \mathcal{H}_\rho(u, x_i) = 1 \quad \text{for any node different from } x_S, \\ \\ u(x_S) = 0. \end{cases} \tag{5.13}$$

Here, the numerical Hamiltonian is the Godunov Hamiltonian for $H(x,p) = ||p|| - 1$.

For any mesh points x_i and x_j, we consider a path $P(x_i \to x_j) = x_i \dots P_k \dots x_j$ connecting x_i and x_j. The points P_k of $P(x_i \to x_j)$ are nodes of the mesh. We define $\#(P(x_i \to x_j))$ as the number of nodes that define the path $P(x_i \to x_j)$. We consider u defined by

$$u^e(x_i) = \min_{P(x_i \to x_S))} \left(\sum_{l=1}^{\#(P(x_i \to x_S))} P_l P_{l+1} \right), \tag{5.14}$$

with the convention $P_1 = x_i$ and $P_{\#(P(x_i \to x_S))} = x_S$.

LEMMA 5.1. *Let $k \geq 0$. We have, for any mesh point x_ℓ,*

$$\tau_\rho^e(x_i) = \min_{P(x_i \to x_S)} \left(\sum_{l=0}^{\#(P(x_i \to x_S))} P_j P_{j+1} + \tau_\rho^e(x_\ell) \right).$$

Proof. Let P be an optimal path that connects x_ℓ to x_S, and P' be a path that connects x_i to x_ℓ. The path $P \cup P'$ connects x_i to x_S, and we have

$$\tau_\rho^e(x_i) \leq \sum_{j=1}^{\#(P(x_i \to x_S))} P_j P_{j+1} + \tau_\rho^e(x_\ell).$$

By taking the infinum, we have the first inequality. Let P now be an optimal path for

$$v(x_i) = \min_{P(x_i \to x_\ell)} \left(\sum_{l=0}^{\#(P(x_i \to x_S))} P_j P_{j+1} + \tau_\rho^e(x_\ell) \right).$$

If P' is an optimal path for $u(x_\ell)$, by connecting the two paths, we get the opposite inequality. ∎

We show that τ_ρ^e defined in (5.14) is a supersolution of the problem. First it is clear that $u(x_S) = 0$. For any node x_i, we denote by $\mathcal{N}(x_i)$ the neighboring nodes of x_i in the mesh. We show now that

$$\max_{x \in \mathcal{N}(x_i)} \left(\frac{\tau_\rho^e(x_i) - \tau_\rho^e(x)}{||x_i - x||} \right) \geq 1. \tag{5.15}$$

This is a direct consequence of Lemma 5.1. Since $\mathcal{H}_\rho \geq \max_{x \in \mathcal{N}(x_i)} \left(\frac{\tau_\rho^e(x_i) - \tau_\rho^e(x)}{||x_i - x||} \right)$,[3] the function τ_ρ^e is a supersolution of (5.12) when $n \equiv 1$.

5.2.2. Study of the scheme (5.12). For any $K > \max_\Omega n(x)$, we consider the scheme (5.12). By using the maximum principle, it is easy to get the next result.

PROPOSITION 5.2. *Under the CFL restriction $\frac{\Delta t}{h} \leq 1/2$, the numerical values $(u_i^n)_{x_i, n \geq 0}$ satisfy the following:*

- *at the source point x_S, $u_{x_S}^n = 0$ for any $n \geq 0$.*

[3] This is true because on each angular sector the maximum is reached by one of the terms $\frac{\tau_\rho^e(x_i) - \tau_\rho^e(x)}{||x_i - x||}$ for $x \in \mathcal{N}_i$ or by the gradient of τ_ρ^e in this angular sector. If we take $\vec{e} = \frac{x - x_i}{||x - x_i||}$, we have $\frac{\tau_\rho^e(x_i) - \tau_\rho^e(x)}{||x_i - x||} \leq |\,(Du \mid \vec{e})\,| \leq ||D\tau_\rho^e||$, and the inequality follows.

- $0 \leq u_i^n \leq K\tau_\rho^e(x_i)$ *for any* x_i, $t_n = n\Delta t$.
- *For any* i, *the sequence* (u_i^n) *has a limit when* $n \to +\infty$, *which is the solution of*

$$\begin{cases} \mathcal{H}_\rho(D_{T_1}u, \dots, D_{T_1}u) - n(x_i) = 0 & \text{for any } x_i, \\ u_{x_S} = 0 & \text{at } x_S, \\ \max\left(\mathcal{H}_\rho^b(D_{T_1}u, \dots, D_{T_1}u) - n(x_i), K\tau_\rho^e(x_i)\right) & \text{on the boundary.} \end{cases}$$

In particular, u_i^n is *independent* of K and ρ when $K \geq \max_\Omega n(x)$.

Proof.

- $0 \leq u_i^n$. This is obvious since the scheme is monotone and $u_i^0 = 0$.
- $u_i^n \leq K\tau_\rho^e(x_i)$. The previous results show that $K\tau_\rho^e$ is a supersolution of (5.12) when $K \geq \max_\Omega n(x)$. The uniqueness principle shows that $u_i^n \leq K\tau_\rho^e(x_i)$.
- At the source point, $u_{x_S}^n = 0$. This is true for $n = 0$. Assume that $u_{x_S}^n = 0$. Since $0 \leq u_i^n$, and thanks to the monotonicity property of $\mathcal{H}_\rho$, we have $\mathcal{H}_\rho \leq 0$ at x_S. Since $\tau_\rho^e(x_S) = 0$, we have

$$u_{x_S}^{n+1} = \min(-\Delta t\mathcal{H}_\rho + \Delta t n(x_S), 0) = 0.$$

The last statement is obvious by continuity. ∎

By applying the result of Theorem 2.2, we conclude the following.

PROPOSITION 5.3. *The solution of the scheme*

$$\begin{cases} \mathcal{H}_\rho(D_{T_1}u, \dots, D_{T_1}u) - n(x_i) = 0 & \text{for any } x_i, \\ u_{x_S} = 0 & \text{at } x_S, \\ \max\left(\mathcal{H}_\rho^b(D_{T_1}u, \dots, D_{T_1}u) - n(x_i), K\tau_\rho^e(x_i)\right) & \text{on the boundary} \end{cases}$$

converges, as $\rho \to 0$, *to the function* (5.9) *when* Ω *is smooth enough.*

5.2.3. Numerical application. We have considered in numerical applications [2] the index n given by a realistic model of the underground of the Gabon gulf, the Marmousi model developed by the French Petroleum Institute (IFP). Since there is no exact solution in closed form for this problem, it is probably more enlightening to consider a more academical problem where an exact solution is known. The computational domain is represented in Figure 14, and the solution at any point M is the distance between the point S and M. A mesh is displayed in Figure 15. The numerical solution is shown in Figure 16. The boundary conditions are very well taken into account: there is no boundary layer, and the isolines of the solution are orthogonal to the circle, as they should be. In Figure 17, we display the isolines of the logarithm of the error between the exact and the computed solutions.

6. Conclusion and summary. In this paper, we have described two ways of discretizing boundary conditions for first order Hamilton–Jacobi equations for which convergence can be proved. This is done through a boundary numerical Hamiltonian. In the case of convex or concave Hamiltonians, we have given explicit formulas. In the case of a coercive Hamiltonian, we have shown that the natural boundary conditions prevent the appearance of numerical boundary layers. Then we have illustrated the schemes by simple numerical examples. An extension to geophysics is also provided.

Appendix A. Some properties of monotone numerical schemes. The aim of this section is to provide some properties of the maximum principle type for monotone numerical schemes:

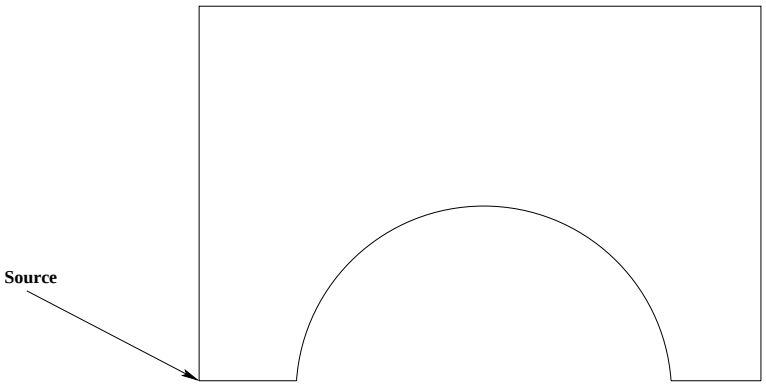

FIG. 14. *Test case for the Soner/source boundary conditions. The Soner condition is imposed everywhere except at the source.*

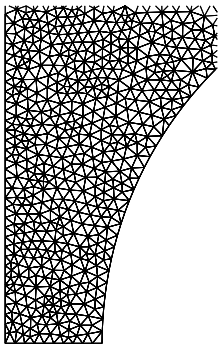

FIG. 15. *Zoom of the mesh around the source. Number of vertices:* 5906; *number of triangles:* 11430.

- For steady problems,

$$\mathcal{H}_\rho(x_i, u_i^n, \{u_j^n, j \in \mathcal{N}_i\}) = 0. \tag{A.1}$$

- For unsteady problems,

$$u_i^{n+1} = G_\rho(x_i, u_i^n, \{u_j^n, j \in \mathcal{N}_i\}; \Delta t) = u_i^n - \Delta t \mathcal{H}_\rho\left(x_i, u_i^n, \{u_j^n, j \in \mathcal{N}_i\}\right). \tag{A.2}$$

These results are useful in section 4. The notation is the same as in section 3.

As in the continuous case, we say that a piecewise linear function u is a discrete subsolution of (A.1) if we have

$$\text{for any } x_i, \quad \mathcal{H}_\rho(x_i, u(x_i), D_{T_1} u, \dots, D_{T_k} u) \le 0.$$

It is a supersolution of (A.1) if

$$\text{for any } x_i, \quad \mathcal{H}_\rho(x_i, u(x_i), D_{T_1} u, \dots, D_{T_k} u) \ge 0.$$

Similarly, let $R > 0$ and $\Delta t \le \Delta t_R$ to ensure the monotonicity of the operator G in (A.2). We say that $u \in \mathcal{C}_R$ is a subsolution of the explicit scheme (A.2) if for all

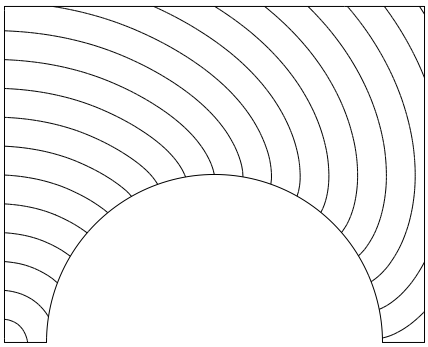

FIG. 16. *Numerical solution.*

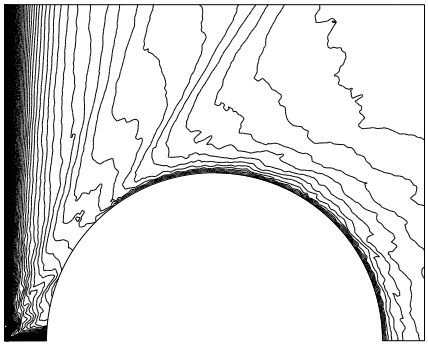

FIG. 17. *Isolines of* $\log_{10}(\tau^{exact} - \tau^{num})$, *max* $= -1.82$.

$n \geq 0$,

$$\text{for any } x_i, \quad \frac{u_i^{n+1} - u_i^n}{\Delta t} + \mathcal{H}_\rho(x_i, u^n(x_i), D_{T_1} u^n, \dots, D_{T_k} u^n) \leq 0.$$

$v \in \mathcal{C}_R$ is a supersolution when the opposite inequality holds. The case of implicit schemes is dealt with the same way.

A solution is obviously a sub- and supersolution, and by maximum principle we understand the following: if u (resp., v) is a sub- (resp., super-)solution of (A.1) such that for any x_i on the boundary of Ω_h we have

$$u(x_i) \leq v(x_i),$$

then the same inequality is true for any node of Ω_h. We say that there is a maximum principle on (A.2) and (A.1) if when u and v are sub- and supersolutions of (A.2) and (A.1) with $u_i^n \leq v_i^n$ on the boundary nodes of Ω_h and for any node of Ω_h at $t = 0$ or t_N, then $u_i^n \leq v_i^n$ everywhere.

We want to show that under the assumptions (H0)–(H1) or (H0)–(H2) below, we have a maximum principle for some classes of schemes of the type

$$G_\rho(x_i, \xi; \{\zeta_l\}_{l \in \mathcal{N}_i}) = 0. \tag{A.3}$$

(H0) The numerical Hamiltonian $\mathcal{H}_\rho$ is monotone increasing in ζ_i and monotone decreasing in $\zeta_l, l \neq i$, for any i. It also satisfies the following: for any i, $\xi \in \mathbb{R}$, and any $(\zeta_1, \dots, \zeta_k)$, $\mathcal{H}_\rho$ is invariant by translation on the ζ_ks.

(H1) For any $R > 0$, for any u, v such that $-R \leq v \leq u \leq R$, for any $p_1, \dots, p_k$ vectors, and for any mesh point x_i, we have

$$\gamma_R(u - v) \leq \mathcal{H}_\rho(x_i, u, p_1, \dots, p_k) - \mathcal{H}_\rho(x_i, v, p_1, \dots, p_k).$$

Here, k is the number of triangles having x_i as vertex.

(H2) The Hamiltonian $\mathcal{H}_\rho$ is convex in the variables $p_1, \dots, p_k$, and there exists a subsolution $\Phi_i, i = 1, \dots, n_s$, and $\alpha < 0$ such that $\mathcal{H}_\rho(x_i, D_{T_1}\Phi, \dots, D_{T_k}\Phi) \leq \alpha$ for any i.

The assumptions (H1) and (H2) are only the discrete analogue of classical assumptions on the Hamiltonian H.

Here, we provide a maximum principle for a monotone Hamiltonian and a *fixed* mesh only. The arguments are too crude to pass to the limit.

A.1. Maximum principle in the steady case.

THEOREM A.1. *We assume that the scheme satisfies* (H0) *and* (H1). *If* $(u_i)_{x_i}$ *and* $(v_i)_{x_i}$ *are sub- (super-)solutions of* (A.3) *in the interior nodes of* Ω_h *and satisfy* $u_i \leq v_i$ *on its boundary nodes, then* $u_i \leq v_i$ *everywhere.*

Proof. Let $R = \max_{x_i, i=1,\dots,n_s}(|u_i|, |v_i|)$ and x_{i_0} be the mesh point where $\{u_i - v_i\}_i$ reaches its maximum. Let us call this maximum M. If x_{i_0} belongs to the boundary, then $M \leq 0$ and we are done. If x_{i_0} is an interior point, then we have

$$\phi = v_{i_0} - u_{i_0} + u = -M + u \leq v$$

on Ω_h, by assumption. Moreover, $\phi(x_{i_0}) = v_{i_0}$.

Since $\mathcal{H}_\rho$ is monotone, we have

$$\begin{aligned} 0 &\leq G_\rho(x_{i_0}, v_{i_0}, v_{i_1}, \dots, vi_k) \\ &\leq G_\rho(x_{i_0}, v_{i_0}, \phi(x_{i_1}), \dots, \phi(x_{i_k})) \\ &= G_\rho(x_{i_0}, \phi(x_{i_0}), \phi(x_{i_1}), \dots, \phi(x_{i_k})) \\ &= \mathcal{H}_\rho(x_{i_0}, D_{T_1}u, \dots, D_{T_k}u). \end{aligned}$$

Then, since u is a subsolution, assuming $M > 0$, we have

$$\gamma_R(u_{i_0} - v_{i_0}) \leq \mathcal{H}_\rho(x_{i_0}, u_{i_0}; D_{T_1}u, \dots, D_{T_k}u) - \mathcal{H}_\rho(x_{i_0}, v_{i_0}; D_{T_1}u, \dots, D_{T_k}u) \leq 0,$$

which is absurd. ∎

THEOREM A.2. *Under* (H0)–(H2), *there is a maximum principle.*

Proof. We consider u and v a sub- and supersolution of $\mathcal{H}_\rho = 0$ with $u \leq v$ on the boundary of Ω_h. We can assume that $\phi \leq v$ on the boundary of Ω_h, thanks to (H0).

Let $\lambda \in [0, 1]$ and $u_i^\lambda = \lambda u_i + (1 - \lambda)\phi_i$. It is clear that u^λ is a subsolution of $\mathcal{H}_\rho = (1 - \lambda)\alpha$ and $u^\lambda \leq v$ on the boundary of Ω_h. Let us assume that $u^\lambda - v$ reaches its maximum C_λ at an interior point x_{i_0}.

By assumption, we have $\mathcal{H}_\rho(x_{i_0}, v_{i_0}, v_{i_1}, \dots, v_k) \geq 0$ and $\mathcal{H}_\rho(x_{i_0}, u_{i_0}^\lambda, u_{i_1}^\lambda, \dots, u_k^\lambda) \leq (1 - \lambda)\alpha < 0$. The same arguments as in the proof of Theorem A.1 show that

$$(1 - \lambda)\alpha \geq \mathcal{H}_\rho(x_{i_0}, u_{i_0}^\lambda, u_{i_1}^\lambda, \dots) \geq \mathcal{H}_\rho(x_{i_0}, u_{i_0}^\lambda, v_{i_1} + C_\lambda, \dots) = \mathcal{H}_\rho(x_{i_0}, v_{i_0}, v_{i_1}, \dots),$$

and we have a contradiction. Thus, $u^\lambda - v$ is maximum on the boundary, and then

$$u^\lambda \leq v$$

in Ω. By taking the limit when $\lambda \to 1$, we conclude that $u \leq v$ in Ω. ∎

A.2. Maximum principle in the unsteady case.

THEOREM A.3. *If the scheme* (A.2) *is monotone under* $\Delta t \leq \Delta t_R$, *then we have a maximum principle. If* $u^n \in \mathcal{C}_R$ *(resp.,* $v^n \in \mathcal{C}_R$*) is a subsolution (resp., supersolution) of* (A.2) *such that* $u_i^0 \leq v_i^0$ *for all* i *and* $u_i^n \leq v_i^n$ *for each* $n \geq 0$ *and boundary node, then* $u_i^n \leq v_i^n$ *for all* $n \geq 0$ *and* i.

The same result holds for an implicit scheme.

Proof. We give the proof for the scheme (A.2). The proof for an implicit scheme is the same. We proceed by induction on n. For $n = 0$, the result is true by assumption. Since $u_i^0 \leq v_i^0$ for the interior points and the boundary points, we have $u_i^1 \leq v_i^1$ for the *interior* nodes. By assumption, $u_i^1 \leq v_i^1$ for the boundary points, and the result follows by induction. ∎

A.3. A uniqueness principle. We consider the scheme

$$\text{(A.4)} \quad \begin{cases} \mathcal{H}_\rho^b(x_i, u_i; u_i, \{u_l, l \in \mathcal{N}_i\}) = 0 & \text{if } x_i \text{ interior node} \\ \\ \max(\mathcal{H}_\rho(x_i, u_i; u_i, \{u_l, l \in \mathcal{N}_i\}), u_i - \varphi(x_i)) = 0 & \text{otherwise,} \end{cases}$$

which discretizes the Dirichlet problem

$$\begin{array}{ll} H(x, u(x), Du(x)) = 0 & \text{if } x \in \Omega, \\ u = \phi & \text{otherwise.} \end{array}$$

We have the following result.

THEOREM A.4. *Under the assumptions* (H0)–(H1) *or* (H0)–(H2) *for* $\mathcal{H}_\rho$ *and* $\mathcal{H}_\rho^b$, *if* u *(resp.,* v*) is a subsolution (resp., supersolution) of* (A.4), *then* $u_i \leq v_i$ *for any mesh point* x_i.

A direct consequence of this result is that if (A.4) has a solution, it is unique.

Proof. We consider $M = \max_{x_i}(u_i - v_i)$, and we assume $M > 0$. Since the set x_i is finite, the maximum is reached at x_{i_0}. If x_{i_0} is not on the boundary, then we can repeat the arguments for the discrete maximum principle. Thus we can assume that x_{i_0} is on the boundary, and we have

$$\begin{array}{l} \max(\mathcal{H}_\rho^b(x_{i_0}, u_{i_0}; u_{i_0}, \{u_l, l \in \mathcal{N}_{i_0}\}), u_{i_0} - \varphi(x_{i_0})) \leq 0, \\ \max(\mathcal{H}_\rho^b(x_{i_0}, v_{i_0}; v_{i_0}, \{v_l, l \in \mathcal{N}_{i_0}\}), u_{i_0} - \varphi(x_{i_0})) \geq 0. \end{array}$$

The conditions on u give

$$\mathcal{H}_\rho^b(x_{i_0}, u_{i_0}; u_{i_0}, \{u_l, l \in \mathcal{N}_{i_0}\}) \leq 0 \quad \text{and} \quad u_{i_0} \leq \varphi(x_{i_0}).$$

Those on v give

$$\mathcal{H}_\rho^b(x_{i_0}, u_{i_0}; u_{i_0}, \{u_l, l \in \mathcal{N}_{i_0}\}) \geq 0 \quad \text{or} \quad v_{i_0} \geq \varphi(x_{i_0}).$$

First case. $u_{i_0} \leq \varphi(x_{i_0})$ and $v_{i_0} \geq \varphi(x_{i_0})$. There is nothing to prove; $M \leq 0$.

Second case. $\mathcal{H}_\rho^b(x_{i_0}, u_{i_0}; u_{i_0}, \{u_l, l \in \mathcal{N}_{i_0}\}) \leq 0$ and $\mathcal{H}_\rho^b(x_{i_0}, u_{i_0}; u_{i_0}, \{u_l, l \in \mathcal{N}_{i_0}\}) \geq 0$. By using the same arguments as in the maximum principle, we get an absurdity when $M > 0$.

Thus we have proved that $M \leq 0$, i.e., $u_i \leq v_i$ for any x_i. ∎

Acknowledgements. A.P. Blanc and G. Barles (University of Tours, France) are acknowledged for many interesting and useful discussions.

REFERENCES

[1] R. Abgrall, *Numerical discretization of first order Hamilton–Jacobi equations on triangular meshes*, Comm. Pure Appl. Math., 49 (1996), pp. 1339–1373

[2] R. Abgrall and J.D. Benamou, *Big ray tracing and eikonal solver on unstructured grids: Application to the computation of a multi-valued travel-time field*, Geophysics, 64 (1999), pp. 230–239.

[3] M. Bardi and S. Osher, *The nonconvex multi-dimensional Riemann problem for Hamilton–Jacobi equations*, SIAM J. Math. Anal., 22 (1991), pp. 344–351.

[4] G. Barles, *Solutions de viscosité des équations de Hamilton–Jacobi*, Math. Appl., Springer Verlag, Paris, 1994.

[5] G. Barles and P.E. Souganidis, *Convergence of approximation schemes for fully nonlinear second order equations*, Asymptot. Anal., 4 (1991), pp. 271–283.

[6] J.D. Benamou, *Big ray tracing: Multivalued travel time field computations using viscosity solutions of the eikonal equation*, J. Comput. Phys., 128 (1996), pp. 463–474.

[7] P.G. Ciarlet and P.A. Raviart, *General Lagrange and Hermite interpolation in $\mathbb{R}^n$ with application to finite element methods*, Arch. Ration. Mech. Anal., 42 (1972), pp. 177–199.

[8] M.G. Crandall and P.-L. Lions, *Two approximations of solutions of Hamilton–Jacobi equations*, Math. Comp., 43 (1984), pp. 1–19.

[9] S. Osher and C.W. Shu, *High–order essentially nonoscillatory schemes for Hamilton–Jacobi equations*, SIAM J. Numer. Anal., 28 (1991), pp. 907–922.